Journal of Electron Spectroscopy and Related Phenomena, 64/65 (1993) 167–175
0368-2048/93/$06.00

The Role of Localized Surface Plasmons in Photoemission from Silver Films: Direct and Indirect Transition Channels

Constantine Douketis, Vladimir M. Shalaev†, Tom L. Haslett, Zhouhang Wang, and Martin Moskovits

Department of Chemistry, University of Toronto and Ontario Laser and Lightwave Research Centre, Toronto, Ontario, M5S 1A1, Canada

We have examined electron photoemission spectra and scanning tunnelling microscopy images from rough (coldly deposited) and smooth (annealed) Ag films. Photoemission is induced by 1-photon and 2-photon processes under conditions of common total photon energy, polarization and light penetration depth. For smooth films we show that photoemission involves direct optical transitions and that the 2-photon excitation is a simultaneous absorption rather than a 2-step process. On rough films the 2-photon process is mediated by the excitation of localized surface plasmon modes, it is strongly enhanced, and it involves indirect, momentum non-conserving transitions. One-photon excitation on rough films is not induced by localized surface plasmons since the frequency of the light falls outside their resonance band. Low temperature scanning tunnelling microscope images of rough films directly show the roughness features on which localized surface plasmon activity is centred.

1. INTRODUCTION

Plasmon excitation in metals is characterized by a modulation of the electronic charge density, sometimes at visible, and often at UV frequencies. One may distinguish between three types of plasmons: 1) bulk plasmons 2) surface plasmons that propagate as two-dimensional waves (SPW) along a surface and 3) localized surface plasmons (LSP) where the modulation of the charge density is spatially restricted to the surface of finite-sized nano-scale particles. LSPs exhibits remarkable characteristics and in this paper we explore some of those characteristics as manifested in photo-induced electron emission from Ag films.

Photoelectron spectroscopy is now an established method for the study of the electronic states of metals and adsorbates. One-photon photoemission has provided detailed information on band structure especially in angle resolved experiments. More recently electron emission has been initiated with multi-photon excitation. This is of interest because the involvement of normally unoccupied intermediate states, found between the Fermi level and the vacuum level, is revealed [1a]. A 3-step model was developed in the mid-sixties by Berglund and Spicer that describes the photoemission process in terms of 1) excitation of the photoelectron 2) migration to the surface while suffering inelastic collisions en route and 3) escape into the vacuum [2]. This model has been used extensively because of its simplicity. Although a 1-step model is currently often used for the description of photocurrents from single crystal surfaces, the 3-step model is still of interest for polycrystalline systems that are of greater practical importance [1b].

There are two important questions one may ask regarding the photoemission process. First, is photoemission initiated by direct optical transitions that conserve electron momentum, or are indirect transitions involved, and under what circumstances does one dominate over the other? Of course, the surface boundary itself acts to break translational invariance and, if photoemission is predominantly a surface effect, the indirect excitation path is favoured. On the other hand, the depth of light penetration into the metal is on the order of tens of nm and, therefore, one might anticipate a strong volume contribution involving direct transitions. Closely related to the first question is the second one: Does the multi-photon excitation that leads to photoelectron ejection involve a true n-photon (simultaneous) absorption or an n-step (cascade)

absorption process?

In this paper we present experimental results and theoretical arguments that distinguish between the above two possibilities. This is achieved by comparing 1-photon and 2-photon electron emission spectra from both rough and smooth Ag films under conditions of constant total photon energy, light penetration depth and light polarization. We find that for smooth films, photoemission is initiated by simultaneous 2-photon, direct transitions. On roughened surfaces, however, we develop a theory, supported by our experiments, that indicates that photoemission is induced largely from the decay of excited LSP modes into 1-electron excitations and involves 2-photon absorption via resonant intermediate states with indirect transitions dominating. We have also recorded scanning tunnelling microscopy images that show a detailed view of the features that support LSP activity.

Ag film surfaces studied in ultra high vacuum are formed by condensation of atomic beams onto a substrate. If the atomic beam condenses on a substrate cooled below 150 K or so it has been postulated that the film surface is characterized by microscopic surface roughness [3]. Following the commonly accepted terms found in the literature, films prepared in this way will be referred to as "rough" films, while Ag films formed at temperatures higher than 250 K, where there is sufficient thermal mobility for self-annealing, will be called "smooth" films. Rough films are known to exhibit an enhanced optical response towards a number of experiments. First, an anomalous optical absorption has been observed as a broad resonance that spans a large part of the visible spectrum [4]. This has been successfully modelled by considering the collective optical response of a rough surface consisting of an assembly of spherical structures between a few nm and tens of nm in diameter [5]; no such anomalous absorption is observed on a smooth film. Second, Raman scattering is strongly enhanced; this has been used to advantage by allowing one to spectroscopically detect the presence of small quantities of adsorbate [6]. Third, second harmonic generation is enhanced [7] as are luminescence and 2-photon fluorescence [8]. Additionally there is interest in unique chemistry, either photo-induced or electron-mediated, that may take place near the surface structures of rough Ag films [9]; the epoxidation of ethylene is one good example. The dominant mechanism for the above effects is thought to involve LSP excitation [3].

Recently, evidence that supports a view of rough Ag surfaces as self-affine fractal systems has been presented [10]. The film may then be viewed as a fractal self-similar arrangement of features each capable of sustaining LSP resonances. We show in Ref. 11 that LSP modes on individual roughness features couple via a dipole-dipole mechanism. This results in an overall modulation of the film surface charge density that is strongly localized spatially. Formally, all roughness features over the entire surface respond to the optical excitation, but the effective modulation of the charge density occurs only in restricted domains of the surface and involves only roughness features within those domains. The coupling scheme that connects the roughness features is certainly not remarkable; rather, it is the self-affine arrangement of roughness features that gives rise to localized excitation zones. Although rough films are, at best, self-affine rather than self-similar, we will assume that the results of Ref. 11 apply to these films as well because the high local fields responsible for surface enhanced optical phenomena are a consequence of mode localization [12].

In a previous paper we reported enhanced 2-photon electron emission quantum yields from rough Ag films [13]. At a photon energy of approximately 2.2 eV it was found that the 2-photon quantum yield from rough films exceeded that from smooth films (examined under identical ultra high vacuum conditions) by up to a factor of several thousand. This enhancement was ascribed to LSP excitation. Here we present energy resolved photoelectron data obtained with laser-excited time-of-flight electron energy analysis from similar Ag film systems. The present data provide strong evidence that LSPs are key participants in the 2-photon photoemission process occurring on roughened surfaces.

2. THEORY

In this section we present the essential points of a theory that explains the linear and non-linear

photoelectric response of the energy resolved studies we have conducted. We will show that photoemission is distinctly different when the excitation frequency of the laser falls within the LSP resonance profile.

Considering that the wave vector of the incident light, **q**, is much less than the electron momentum, **k**, the spatial dependence of the exciting radiation field can be neglected. The interaction operator is $(e/2mc)[\hat{A}\hat{p} + \hat{p}\hat{A}]$ for transitions between Bloch states and the matrix elements are nonzero only for direct electron transitions between those states. Since the light penetrates tens to hundreds of atomic layers, while translational invariance is broken only for few atomic layers near the boundary, photoemission in smooth films can be, and has been, successfully interpreted in terms of direct transitions in the bulk [14].

Koyama and Smith [14] have used the two-orthogonal plane wave approximation (2-OPW) to describe the 1-photon photoeffect in Ag. We are presently preparing a publication [15] that extends this approach to include 2-photon excitation in complete detail. That work also details the development of simple expressions for $P(E,\omega)$, the number of excited electrons per unit time, unit volume, and unit energy interval for both 1-photon and 2-photon excitation in smooth and rough films. $P(E,\omega)$ is proportional to the photoemission probability which, in turn, is proportional to the experimentally measured electron energy distribution curve (EDC).

We show in Ref. 15 that for a 1-photon process in a polycrystalline smooth film:

$$P^{(1p)}(E,\omega') = \frac{n_G}{24\hbar\pi}\left(\frac{eE^{(0)}}{\hbar\omega'}\right)^2 \times \frac{G}{1-\gamma}\left(\frac{V_G}{\hbar\omega'}\right)^2 \qquad (1)$$

G is the reciprocal lattice vector, $2V_G$ is the L_2' to L_1 energy gap, n_G is the number of symmetrically equivalent G planes, $E^{(0)}$ denotes the radiation field strength at photon energy $\hbar\omega'$ and $1-\gamma = [(\hbar\omega')^2 - 4V_G^2]^{1/2}/\hbar\omega'$. As outlined in Ref. 14, $P^{(1p)}(E,\omega')$ is non-zero only within the energy interval $E_{min} < E < E_F$, where $E_{min} = [(\hbar\omega' - (\hbar^2/2m)G^2)^2 - 4V_G^2]/[2(\hbar^2/m)G^2]$, m being the electron mass, and E_F is the Fermi energy. Multiplying $P^{(1p)}(E,\omega')$ by the electron transmission and the electron escape functions produces a quantity proportional to the EDC. The electron transmission function is essentially constant over the narrow range of electron energies studied here. On the other hand, the escape function takes the form $T_0(E) = \frac{1}{2}\{1-[(E_F+\Phi)/E]^{1/2}\}$ for $E > E_F+\Phi$ and is zero otherwise [2]; Φ is the work function.

In Fig. 1 we present the band structure of Ag in the vicinity of the L symmetry point to illustrate the type of transitions leading to photoemission that can take place. The two conduction bands shown are calculated using the fully relativistic augmented plane-wave method described by Christensen [16]. The dispersion curves are scaled so that E_F is 0.3 eV above the L_2' saddle point and $2V_G$ is 4.15 eV; this scale restriction is imposed so that the curves agree with piezo-reflectance

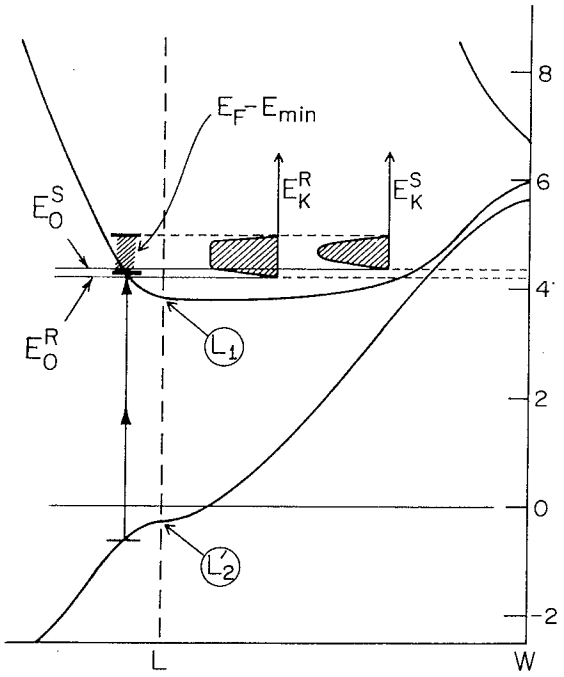

Fig. 1. Band structure of Ag near the L symmetry point. Direct 1-photon or 2-photon transitions at 4.85 eV total energy are shown as the vertical arrows on the left. The energy scale is in units of eV with the origin at the Fermi level.

measurements [17]. Two vacuum levels are included, E_0^R and E_0^S, corresponding to the two values of the work function that we have measured for rough and smooth Ag films [13]. At our photon energy it is possible to draw only one direct transition on this diagram; it is shown slightly displaced to the left of the L point. Other possible direct transitions of constant interband energy can be represented in a 3-dimensional view of the band structure that extends in front of and behind the plane of the paper (Fig. 1 is a cross-section of the band structure surface). In accordance with Koyama and Smith, those transitions are all incorporated within the range E_F-E_{min}=0.67 eV indicated by the shaded region in the figure (the value of 0.67 eV has been calculated using the piezo-reflectance data and assuming **G** to be along <111> [14]). Schematic representations of photoemission spectra for rough and smooth films are included in Fig. 1 to illustrate that photoemission signal is observed within an energy window allowed by the rectangular shaped box bounded by E_F-E_{min}.

For direct, 2-photon excitations in the $L_2' \rightarrow L_1$ region of Ag with $\omega = \omega'/2$ we have determined $P^{(2p)}(E,\omega)$ to be [15]:

$$P_S^{(2p)}(E,\omega) = \frac{n_G}{20\pi(1-\gamma)} \frac{(eE^{(0)})^4 G}{m\hbar^4\omega^5} \times \left(\frac{V_G}{\hbar\omega}\right)^2 \left(\frac{V_n}{\hbar\omega}\right) \tag{2}$$

in the range $E_{min} < E < E_F$ and zero otherwise. $V_n = \hbar^2 k_n^2/(2m)$ where k_n is the radius of the Fermi surface "neck". We assume throughout that we are near threshold. This function (Eq. 2) is also box-like. It too must be multiplied by $T_0(E)$ to give the 2-photon EDC.

Our model of the rough film is based on a fractal arrangement of polarizable objects [11,12]. The field close to a surface roughness feature (the near zone) is given by $E_\alpha^{(nz)} = E_\beta^{(0)} r^{-3}(\delta_{\alpha\beta} - 3n_\alpha n_\beta)\eta_{\beta\beta}$, where **r** is a position vector originating at the centre of the roughness feature, **n** = **r**/r, and η is the polarizability of the roughness feature. The Fourier transform of $E_\alpha^{(nz)}$ includes components with high **q** values, even comparable to **k**. This breaks translational symmetry and weakens the momentum conservation requirement. Because the fields in the near-zone are enhanced compared to the incident field, photoemission from rough films will be dominated by transitions (which need no longer be direct) initiated by the absorption of photons within the rapidly varying fields of the near-zone.

For direct electron transitions, the matrix elements $V_S \sim eE^{(0)}k(\hbar/m\omega)$. The corresponding matrix elements for a rough film, V_R, include contributions from all transitions, even those with a change in momentum as large as $|G| \approx a^{-1}$. In Ref. 15 we show that $V_R/V_S \sim (a/R_0)^2(R_0^3/v_{loc})\chi$ where R_0 is the linear size of the roughness feature, v_{loc} is the volume within which the electron is localized, $\chi \sim \eta/R_0^3$ is the susceptibility associated with dipolar modes on the roughness features, and *a* is the lattice constant. At resonance $\chi \sim Q$, where Q is the quality factor. For noble metals $Q \sim 10^2$ and the ratio V_R/V_S is close to unity if $v_{loc} \sim R_0^3$.

Assuming that for a rough film V_R is completely independent of $\Delta\mathbf{k}$, one finds:

$$\frac{P_R^{(2p)}(E,\omega)}{P_S^{(2p)}(E,\omega)} \sim \left\langle \frac{a^3}{V} \left| \chi \left(\frac{a}{R_0}\right)^2 \frac{R_0^3}{v_{loc}} \right|^4 \right\rangle (\hbar\omega)^4 \times D_i(E_i) D_m(E_i+\hbar\omega) D_f(E_i+\hbar\omega') \times \left[\frac{2}{\hbar\Gamma_{mm}} + D_m(E_i+\hbar\omega)\right] \tag{3}$$

where *V* is the sample volume, Γ_{mm}^{-1} is the lifetime in the intermediate state, m, the angle brackets denote an average over the random positions and sizes of the roughness features, and $D_i(E_i)$, $D_m(E_i + \hbar\omega)$, and $D_f(E_i + \hbar\omega')$ are the density of initial, intermediate and final states respectively. In contrast to the situation with smooth films (Eqs. 1 and 2), the shape of the EDC is determined by the product of the densities of states. Eq. 3 was obtained by assuming near-threshold excitation and accordingly that $\hbar\omega \sim V_G \sim V_n/(1-\gamma) \sim \hbar^2G^2/(8m)$.

The required average over position is performed implicitly by using the result of Ref. 12 that for fractal structures $\langle|\chi|^4\rangle \sim Q^3$. By estimating the density of states $D \sim (v_{loc}/a^3)E^{-1}$, Eq. 3 reduces to

a simple form which can be used to estimate the roughness-induced photoemission enhancement:

$$\frac{P_R^{(2p)}(E,\omega)}{P_S^{(2p)}(E,\omega)} \sim f(R_S)Q^3(R_S)\left(\frac{a}{R_S}\right)^2 \times \left[\frac{2V_G}{\hbar\Gamma_{mm}} + \left(\frac{R_S}{a}\right)^3\right] . \quad (4)$$

where R_S is the depth of light penetration and $f(R_S)$ is the volume fraction filled by roughness features with size $\leq R_S$. It follows from (4) that roughness features with $R_S \sim R_0$ are predominantly responsible for the photoemission. For Ag at λ = 510 nm, R_S is less than the electron mean free path, l, and Q can be estimated as: $Q(R_S) \sim (R_S/(R_S+l))Q_{bulk}$. Using the following parameters for Ag: a = 4Å, $R_S \approx$ 120Å, l = 400Å, $Q_{bulk} \approx 120$, and assuming that $2V_G/\hbar\Gamma_{mm} \sim 10^2 - 10^4$, and that $f(R_S) \sim 10^{-3} - 10^{-1}$, the enhancement ratio is calculated to lie between 10^2 and 10^4. As indicated in the introduction, in Ref. 13 we experimentally observe a value of several thousand.

3. EXPERIMENTAL

The experiments were carried out in an ultra high vacuum chamber (pumped by a Ti-sublimation pump (550 L/s) and a turbomolecular pump (110 L/s)) at 7×10^{-11} Torr base pressure. Ag films 200 nm thick were deposited at 1×10^{-10} Torr at a rate of 1 nm s^{-1} onto a polished Cu mirror using an effusive beam of Ag atoms. Both interferometric (by detection of the first fringe from a 308 nm laser) and gravimetric (using a calibrated quartz microbalance) methods were used to verify the deposition rate.

The Cu substrate was thermally connected to a closed-cycle He refrigerator through an intervening slab of sapphire (0.5 mm thick); the sapphire slab allowed the sample to be electrically isolated. Any temperature from 300 K to 30 K could be accessed but the cooling process to the lowest temperature required a 4 hour cool-down time. At 30 K the pressure in the chamber fell to 4×10^{-11} Torr due to cryopumping.

The longitudinal axis of a time-of-flight tube (2.5 cm diameter X 1 m long) was oriented along the surface normal. The mouth of the tube was placed 2 cm from the surface. Standard mu-metal was used to magnetically shield the entire length of the flight tube, but the 2 cm region directly in front of the surface was left unshielded. This establishes a minimum observable kinetic energy of 0.5 eV for the spectrometer; slower electrons are deflected by the earth's magnetic field to the extent where they ground out against the walls of the flight tube before reaching the detector.

In order to observe near threshold photoelectrons, a +2.00 V bias (V_B) was applied to the time-of-flight tube. In the observed spectra the low energy cut-off is given by $\Phi_{S,R}-\Phi_A+V_B$ where $\Phi_{S,R}$ and Φ_A are the work functions of the smooth or rough surfaces, and the detector surface, respectively. The high energy cut-off is $2\hbar\omega-\Phi_A+V_B$. The photoelectron arrival rate at the microchannel plate detector was limited to a few counts per second. Cubic weighting converted the time-of-flight data to an energy spectrum. No smoothing was used.

Polarized light from a (10 ns pulse width) dye laser or from a second harmonic generator was focused onto the Cu substrate at 35° incidence. The dye laser power was kept below 0.5 μJ/pulse for rough films, and below 20 μJ/pulse for smooth films to prevent space-charge effects. The second harmonic light power was severely attenuated to give similarly low count rates. At 510 nm (dye laser) and at 255 nm (doubler) the penetration depth of light in Ag is 12.4 nm and 14.0 nm respectively, based on well-known optical constants [18].

Photoelectron spectra for smooth films were recorded at room temperature immediately after deposition and at approximately half hour intervals during the four hour cool-down period to 30 K. A slight lowering of Φ_S (about 0.1 eV) was observed during cool-down due to adsorption of background gasses in the vacuum system (mostly H_2O). The smooth Ag films were then dosed with H_2O to reduce Φ_S further, thereby increasing the energy window within which photoelectric signal appears. Only the low energy cut-off shifts on dosing; the high energy cut-off remains fixed indicating that Φ_A is not affected. Step-wise dosing with H_2O to a total of 5 L (about 5 monolayer) reduced the low energy cut-off by 0.6 eV beyond which no further

change was observed. H_2O does not have any electronically excited states that are accessible with the laser excitation used. Therefore, its presence does not affect the shape of the photoelectron spectrum. Moreover, similar results were obtained with other physisorbed molecules. Photoelectron spectra for rough films were recorded at 30 K immediately after deposition.

In order to avoid space-charge effects the signal levels were kept low, such that a reasonable signal-to-noise ratio of 3 to 5 could be attained in a period of tens of minutes acquisition time. At this low sinal-to-noise level it is not appropriate to normalize spectra at peak values of the data points. Rather, we chose to normalize the data by simply matching peak intensities for smooth lines passed through the data points by eye. Those lines are not shown in the spectra to follow.

Scanning tunnelling microscopy was performed on the Ag films with a new apparatus to be described in detail in a future publication [19]. Briefly, the apparatus consists of an ultra high vacuum chamber containing a tunnelling microscope and a cryostat. The tunnelling tip is fastened to the end of a piezo-electric cylinder (fine tuned x, y and z motion) which, in turn, is connected to a commercial drive for long-range z-direction approach (Burleigh Inc. Inchworm). The sample is mounted on a rotating stage so that Ag atoms can be deposited and then the sample rotated for interrogation by the tunnelling tip. The sample is in good thermal contact with a cryogenic fluid dewar via two flexible Cu ribbons, and thermally isolated from the mount with insulating rods. This allows us to cool the sample to 100 K using liquid nitrogen in the dewar. The tunnelling assembly is vibrationally isolated from the chamber through standard o-ring loops and the chamber is, in turn, mounted on a massive stone slab and vibrationally isolated from the floor with air suspension legs. We have recorded high quality graphite images showing single atom resolution at 100 K. Noise induced by cryogenic fluid bubbling is not a problem. Thermal drifts are found to be minimal over the time taken to record an image (5-10 min).

4. RESULTS AND DISCUSSION

In Fig. 2 we present 1-photon and 2-photon spectra of a smooth film at room temperature (2a) and at 30 K dosed with 5 L H_2O (2b), and of a rough film at 30 K (2c). The 1-photon and 2-photon spectra of a smooth film are identical within the signal-to-noise level. This is the expected spectrum for photoemission initiated by direct transitions for which the EDC is a product of a "rectangular" $P(E,\omega)$ with a "triangular" $T_0(E)$ function [14]. However, the influence of $T_0(E)$ is not apparent in the smooth film spectrum of Fig. 2a because of the narrow energy range within which photoelectron signal appears; in Fig. 2b, this range (or photoelectric window) is extended through lowering of Φ_S by dosing with H_2O, and $T_0(E)$ shows up; it is included as a dashed line in Fig. 2b. The good agreement between the predicted and observed shape of the EDCs suggests that photoemission from a smooth film is initiated by direct (and simultaneous) transitions in the bulk metal both for the 1- and the 2-photon processes. For the 1-photon process this conclusion is not new since no 1-electron transitions are observed in the absorption spectrum of Ag below the plasma edge at approximately 3.8 eV [16]. The weak absorption of Ag in the visible is due entirely to the Drude response.

The 1-photon and 2-photon spectra of a rough Ag film, shown in Fig. 2c, are strikingly different from those of the smooth films. The 1-photon spectrum is largely triangular in shape and resembles the smooth film EDCs. However, there is a small positive departure from the triangular shape that is clearly evident. The 2-photon spectrum is distinctly rectangular; this shape was reproduced with many films of varying thickness. It is found to be weakly dependent on the presence of adsorbate and is independent of light polarization. These observations can be understood by assuming the 1-photon response in rough films to be due to direct transitions while the 2-photon response originates from LSP-mediated, indirect transitions.

The roughness features that support LSP activity in rough Ag films are observable in low temperature scanning tunnelling micrographs. In Fig. 3a an image of a smooth film is shown. This image remains the same whether the film is at

300 K or at 30 K. Some structure is evident in the form of surface undulations of size on the order of 100 to 200 nm. In sharp contrast to this, a similar micrograph of a rough film is shown in Fig. 3b. There, spheroidal structures on a much smaller size range, from 5-20 nm, are evident. These roughness features do not exist at temperatures higher than 150-200 K due to thermal self-annealing of the film. We believe that it is on the roughness structures of Fig. 3b that LSP excitation is centred. The direct observation of the roughness features on a rough Ag film has given us a very good estimate of their size range. Previously we used a value of 12 nm in calculating the photoemission enhancement ratio between a rough and smooth Ag film. The resultant ratio was found to be in excellent agreement with experiment, and

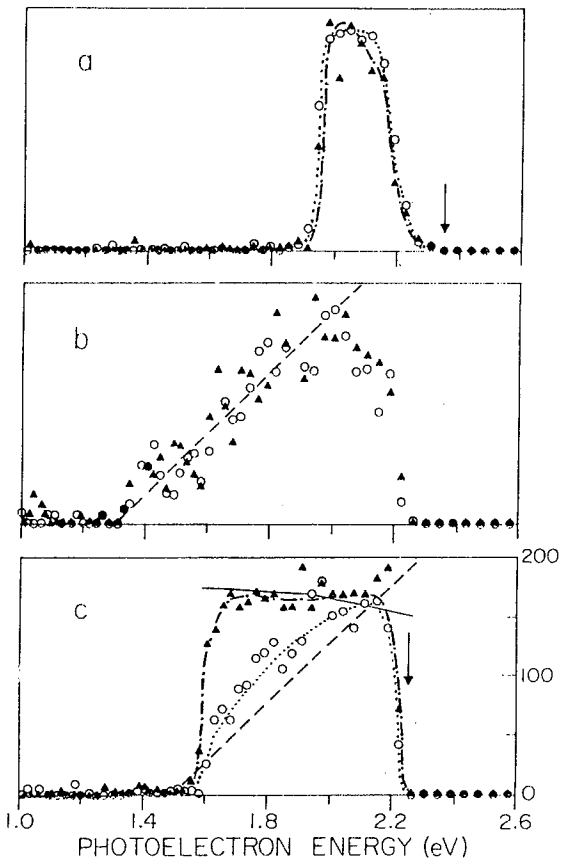

Fig. 2. Normalized 2-photon spectra (triangles and dash-dot line) and 1-photon (open circles and dotted line) spectra for (a) a smooth Ag film at room temperature, (b) a smooth film at 30 K dosed with 5 L H_2O, and (c) a rough film at 30 K. The dotted and dot-dash lines joining the data points in (a) and (c) are only a guide to the eye. The dashed line in (b) and (c) is $T_0(E)$. The solid line in (c) is the DOS product, $D_i(E_i)D_m^2(E_i + \hbar\omega)D_f(E_i + 2\hbar\omega)$. The right-hand ordinate in (c) refers to this DOS product in units of Ry^{-4} $atom^{-4}$.

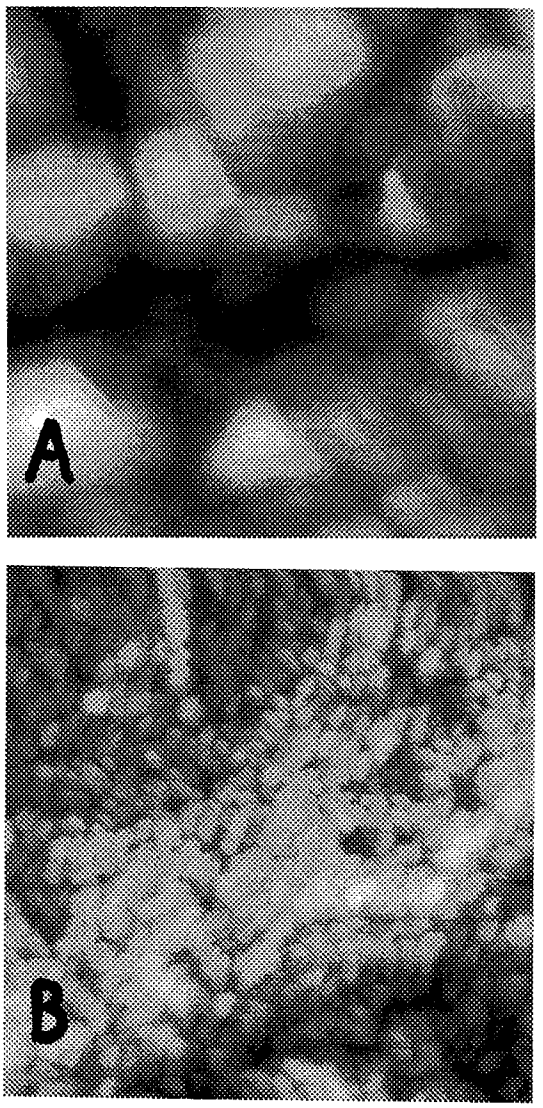

Fig. 3. Scanning tunnelling microscope images of A) a 200 nm thick smooth Ag film deposited at 300 K and imaged at 100 K, and B) a 200 nm thick rough film deposited at 100 K. Both images span a 500 nm X 500 nm domain.

the size used in the calculation is certainly validated by the STM results.

As indicated in the theory section, the local fields around the roughness structures are rapidly varying due to their small size; this breaks symmetry and leads to an enhancement in photoemission by turning on indirect transitions. Additionally, further photoemission enhancement is realized through the localization of the excitation on the extended rough surface.

According to Eq. 3, $P(E,\omega)$ should follow the product $D_i(E)D_m^2(E+\hbar\omega)D_f(E+2\hbar\omega)$, which is drawn as the solid, nearly horizontal line in Fig. 3c, as outlined above. (The second term in the square brackets of (3) usually exceeds the first term.) It is seen that the appearance of the 2-photon EDC is very well explained by the density of states product but only in the absence of any modification from $T_0(E)$. This implies that essentially all of the photoelectrons originate, in this case, near the surface of the roughness features where the field enhancement is largest. A more detailed view of the density of states of Ag is shown in Fig. 4. It is seen that there is a significant variation in the initial, intermediate and final density of states with energy. However, the increase in the initial and final state densities is compensated by the decrease in the intermediate density so that the above product is essentially flat across the region of interest. Note that in Fig. 4 the ordinate does not begin at 0 so that the variations in the density of states are exaggerated.

That LSP excitation in rough films is only observed with visible photons is consistent with the report of an anomalous visible absorption in roughened Ag that has been ascribed to surface plasmon excitations [4,5,11]. The nearly triangular 1-photon response in Fig. 2c shows that direct transitions do take place in rough films when there is sufficient detuning from the LSP resonance. The small departure of the 1-photon EDC from the purely triangular shape observed with smooth films suggests (not unexpectedly) that for rough films a greater fraction of even 1-photon induced electron emission comes from the surface region. The photoemission spectra of the rough films are not affected by the polarization of the laser, apart from the trivial Fresnel reflectivity effect. This is entirely consistent with LSP excitation in surface roughness

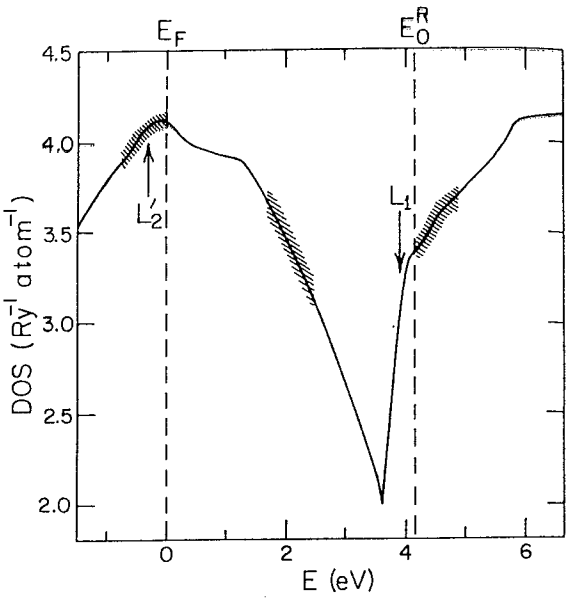

Fig. 4. Density-of-states in $Ry^{-1}atom^{-1}$ for Ag calculated according to Ref. 16. The Fermi level and vacuum levels indicated are for a rough film. The initial, intermediate, and final states involved in photoemission at the photon energies used here are shown as the shaded regions.

and is well known in other experiments, for example, SERS [4].

The difference between the two spectra of Fig. 2c might also be explained in terms of roughness-induced surface states. We believe this to be a less likely explanation because surface states are expected to be strongly polarization dependent and sensitive to adsorption contrary to what is observed. Furthermore, electron energy loss studies [20] and inverse photoemission measurements comparing rough and smooth [21] Ag show no evidence of surface states. Both studies show the bulk electronic structure of rough and smooth Ag films to be very similar. Our results support that conclusion. We see that the EDC cut-off points predicted by the upper limit of the range E_F-E_{min} (indicated by the two vertical arrows in Figs. 2a and 2c) are in good agreement with the high energy extreme of the observed EDCs of both films.

5. CONCLUDING REMARKS

We have presented a unique photoemission study comparing 1-photon and 2-photon spectra of rough and smooth Ag films under conditions of equal total photon energy and nearly equal optical penetration depth. Our findings are consistent with a theory that incorporates the involvement of LSP excitation into existing and well-developed theories of photoemission from metals. We interpret photoemission from smooth films as a process involving direct optical transitions. On rough films, however, where LSP resonances are excited, photoemission is dominated by the enhanced near-zone fields around surface roughness features where translational invariance breaks down. This, together with localization due to the fractality of the rough surface, leads to the conclusion that most of the photoelectrons originate from restricted regions of the irradiated surface. Using this theoretical framework we have estimated an enhancement factor that agrees very well with experiment. The theory outlined extends the 3-step photoemission model to encompass 2-photon excitation.

We have also shown the first STM images of the structures on a rough film that support LSP oscillations. The structures found to be of a size in agreement with theoretical estimates that correctly describe rough film enhancement effects. It would be fascinating to explore the photoelectric response of these films locally by looking for a laser-induced tunnelling current while maintaining the position of the tunnelling tip on a single roughness feature. This and other related experiments, such as examining the extent of roughness as a function of deposition temperature and film thickness, are presently being planned.

We are grateful to NSERC for their financial support and to Mr. Valery Smelyansky for kindly supplying us with his band structure calculations.

†Present address: Department of Physics, New Mexico State University, Las Cruces, NM 88003.

REFERENCES

[1] a) K. Giesen, F. Hage, F.J. Himpsel, H.J. Riess and W. Steinmann, Phys. Rev. Lett. **55**, 300 (1985). b) Topics in Appl. Phys.:Photoemission in Solids, Vol.26, M. Cardona and L. Ley eds., Springer-Verlag (1978).

[2] C.N. Berglund and W.E. Spicer, Phys. Rev. **136**, 1030 (1964).

[3] M. Moskovits, Rev. Mod. Phys., **57**, 783 (1985).

[4] Y. Borensztein, M. Jebari, G. Vuye and T. Lopez-Rios, Surf. Sci. **211/212**, 775 (1989).

[5] P.H. McBreen and M. Moskovits J. Appl. Phys. **54**, 329 (1983).

[6] J.P. Heritage, A.M. Glass, Nonlinear Optical Effects, in "Surface Enhanced Raman Scattering", Eds: R.K. Chang and T.F. Furtak, Plenum Press, N.Y., 1982.

[7] C.K Chen, A.R.B. deCastro, Y.R. Shen, Phys. Rev. Lett., **46**, 145 (1981).

[8] A.M. Glass, P.F. Liao, J.G. Bergman, D.H. Olson, Opt. Lett., **5**, 368 (1980).

[9] G.M. Gouncher, C.A. Parsons, C.B. Harris, J. Phys. Chem., **88**, 4200 (1984).

[10] R. Chiarello, V. Panella, J. Krim, C. Thompson, Phys. Rev. Lett. **67**, 3408 (1991).

[11] M.I. Stockman, T.F. George, and V.M. Shalaev, Phys. Rev. B **44**, 115 (1991).

[12] M.I. Stockman, V.M. Shalaev, M. Moskovits, R. Botet, T.F. George, Phys. Rev. B **46**, 2821 (1992).

[13] J.T. Stuckless and M. Moskovits, Phys. Rev. B **40**, 9997 (1989).

[14] R.Y. Koyama, N.V. Smith, Phys. Rev. B **2**, 3049 (1970).

[15] V.M. Shalaev, C. Douketis and M. Moskovits, in preparation.

[16] N.E Christensen, Phys. Stat. Sol. B **54**, 551 (1972).

[17] C.E. Morris and D.W. Lynch, Phys. Rev. **182**, 719 (1969).

[18] P.B. Johnson and R.W. Christy, Phys. Rev. B **6**, 4370 (1972).

[19] Z. Wang, C. Douketis, T. Haslett and M. Moskovits, in preparation.

[20] R.A. Wolkow and M. Moskovits, J. Chem. Phys. 96, 3966 (1992).

[21] (a) A. Otto, K.H. Frank and R. Reihl, Surf. Sci. **78**, 591 (1978); (b) R. Reihl and R.R. Schlittler, Phys. Rev. B **29**, 2267 (1984).